A simplified model for the determination of current-voltage characteristics of a high pressure hydrogen plasma arc

Papa Gueye, Yann Cressault, Vandad-Julien Rohani, Laurent Fulcheri

A simplified model for the determination of current-voltage characteristics of a high pressure hydrogen plasma arc

P. Gueye[1], Y. Cressault[2], V. Rohani[1] and L. Fulcheri[1]

[1] *MINES ParisTech, PSL-Research University, PERSEE Centre procédés, énergies renouvelables et systèmes énergetiques, CS 10207 rue Claude Dauness 06904 Sophia Antipolis Cedex, France*
Tel : +33.493.957.540, Email : papa.gueye@mines-paristech.fr

[2] *Université de Toulouse, UPS, INPT, LAPLACE (Laboratoire Plasma et Conversion d'Energie), 118 route de Narbonne, F-31062 Toulouse Cedex 9, France*
Tel : +33.561.558.221, Email : cressault@laplace.univ-tlse.fr

Abstract

This paper focuses on the modeling of a hydrogen arc column at very high pressure (20 bar). The problem is solved from Elenbaas-Heller equation where radiation is carefully considered with the net emission coefficient. The absorption spectrum requires the integration of background continuum, molecular bands and line spectra. This work directly aims to predict the electric current-voltage characteristics which is key for the design of new processes. We propose also a new analytic solution which generalizes the channel model of electric arc to the case when the volume radiation makes a significant contribution to the energy balance. The presented formalism allows a better determination of the plasma thickness parameter R_p for net emission coefficient method in cylindrical arcs and gives satisfactory results in comparison to earlier experimental works on high pressure hydrogen plasma.

Keywords: channel arc model, radiation, hydrogen plasma, very high pressure

Introduction

With the present context of fossil fuel depletion, global warming and other major environmental impacts, the energy sector definitively remains one of the most critical. The future of humanity will certainly depend on our ability, during the next decades, to develop new and sustainable solutions in the field of energy.

In the perspective of a foreseeable large scale deployment of renewable energy for electricity production, plasma processes could lead to breakthroughs with new and environmental-friendly processes likely to answer tomorrow's challenges through the replacement of a number of combustion based processes. Indeed, plasma can favorably act as a robust tunable enthalpy source without direct CO_2 emissions while significantly improving the reactivity of number of chemical reactions.

PERSEE group at MINES ParisTech has been working on the plasma-assisted conversion of hydrocarbons. This led to the development of a three-phase AC plasma torch which attains pre-industrial size and runs at atmospheric pressure with different pure and mixture gases (argon, helium, nitrogen, air,...) [1–3]. Studies are also conducted for its improvement toward a very high operational pressure (up to 20 bar) with pure hydrogen.

Very few works has been done on very high pressure thermal plasmas running with hydrogen. To the authors' knowledge, their use refers back to the 70's when the arc heater was developed for the simulation of high temperature re-entry of ballistic missiles in USA [4]. Such scarcity can be explained by the necessity, at 20 bar for example, to design an appropriate power supply, to better calculate the radiative contribution and have materials that resist to high thermal and mechanical constraints.

Deriving the electric characteristic of the arc for power supply specifications is then one first challenge when using hydrogen, known to have a higher voltage than argon, nitrogen, etc. While advanced computational methods as CFD, MHD are costly, there are simplified models such

as channel arc models that give reliable results and have proven to compare well with experiments [5–7].
The approach developed in this paper is crucial when one is willing to derive the current/voltage characteristic of the arc, for a better specification of the power supply at very high pressure. A particular attention is paid to the radiative heat transfer through costly but precise computations of the absorption coefficients [8] used in net emission coefficient (NEC) method.
As in most numerical approaches, physical parameters must be assigned definite values before the program can be run. The plasma thickness appearing in NEC approach was observed to have a great effect on the electric characteristic. Then, for design purposes, a clear understanding of how the input values affect the end result is of great importance. There will be a much greater understanding on this score with an analytic solving. Consequently, one purpose of this paper is also to fix the aforementioned radiative parameter through a new and original formalism for an analytic solution of the energy balance equation. Such modeling of the divergence of the radiative flux as function of the heat flux potential enables to treat almost totally by analytic means the Elenbaas-Heller equation, notwithstanding its severe non-linearities. Finally, the key outcome of this work is the validation of the pressure effect on the arc voltage with previous works on hydrogen plasma [4, 9].

1. General assumptions

At the outset it should be mentioned that the theory of the arc as developed here entirely disregards any phenomena that are due to the presence of electrodes. Hence we assume that the positive column voltage is much bigger than cathode and anode drops and, as for most situations, this column part of the discharge determines the operational characteristics of the arc. In plasma using inert gases like argon, the electron-neutral energy exchange is less effective and requires high currents and electron densities to reach quasi equilibrium whereas in molecular gases such as hydrogen, the local thermodynamic equilibrium (LTE) is easier to reach, thanks to sufficient electronic densities and moderated temperature and density gradients for small diffusive fluxes [10].

2. Arc modeling

One of the major issues to be dealt with arc plasma is its stability. The easiest solution is to surround the arc with a well-cooled wall that should be able to absorb the energy losses without being destroyed. Several investigators have studied the problem of the approach to the asymptotic column. One of the most striking formulations for tube arc problems is that of Stine [6] which showed particularly good agreement with experiments. We consider here a positive column of arc plasma burning and confined inside a cylindrical tube which walls are maintained at a constant temperature. This boundary condition, with a rotationally symmetric geometry, allows us to formulate the channel arc problem without involving the Steenbeck's minimum principle [11] which mathematical meaning in gas discharge physics has also been questioned [12].
The stronger the confinement, the larger the gradients in the plasma arc. We assume nevertheless that the LTE prevails in the whole paper. This can be justified retrospectively, with relatively low densities and temperature gradients, inducing then small diffusive fluxes.

3. Equations

In order to provide a reasonable description of the manner in which the positive column of a DC arc behaves, it is necessary and sufficient to derive the differential equation that describes the energy-transfer processes within the arc column. The temperature distribution in a long cylindrical steady-state thermal plasma column stabilized by tube walls is described by the well-known

Elenbaas-Heller equation [13], derived in the following sections.

3.1 Electric field

For the steady-state arc, the Faraday's law in cylindrical coordinates (r, θ, z) gives

$$\nabla \times \vec{E} = (\frac{1}{r}\frac{\partial E_z}{\partial \theta} - \frac{\partial E_\theta}{\partial z})\vec{e_r} + (\frac{\partial E_r}{\partial z} - \frac{\partial E_z}{\partial r})\vec{e_\theta} + (\frac{1}{r}\frac{\partial (rE_\theta)}{\partial r} - \frac{1}{r}\frac{\partial E_r}{\partial \theta})\vec{e_z} = \vec{0} \tag{1}$$

The E_θ component and the θ derivatives are null for a symmetry matter. Moreover, the arc column refers to that part of the arc plasma axially invariant. Thus, Eq. (1) reduces to

$$\frac{\partial E_z}{\partial r} = 0 \tag{2}$$

Hence, for the positive column, the electric field is uniform.

3.2 Elenbaas-Heller equation

The DC positive column energy equation is given by

$$\nabla \cdot \vec{q} + \nabla \cdot \left[p\vec{v} + \rho(e + \frac{v^2}{2})\vec{v} \right] - \vec{j} \cdot \vec{E} + \nabla \cdot \vec{q}_{rad} = 0 \tag{3}$$

which contains from left to right one conductive term, two convection terms, the Joule heat term and finally the radiation term. $\vec{q}$, p, $\vec{v}$, e, $\vec{j}$, $\vec{E}$ and $\vec{q}_{rad}$ are respectively the conductive flux, pressure, velocity, enthalpy, electric field and radiative flux. The transport through the electron enthalpy and due to the electron drift is neglected.
Within the current range considered here (up to hundreds of amperes), the cathode jet due to Maecker's effect [14] is negligible, so is the self-magnetic field. Thus any convective contribution of the Lorentz force in the energy balance vanishes. The mean gas velocity v is set to zero due to axisymmetric assumption. The Ohm law can be simply written as

$$\vec{j} = \sigma \vec{E} \tag{4}$$

The radiation term in Eq. (3) is computed using Lowke's approach of the net emission coefficient [15], with the divergence of the radiation flux density $\vec{q}_{rad}$ given by

$$\nabla \cdot \vec{q}_{rad} = 4\pi\epsilon_N \tag{5}$$

More details for the computation of the coefficient ϵ_N will be provided in the next section.
Assuming heat transfer by conduction with the Fourier law

$$\vec{q} = -\kappa \nabla T \tag{6}$$

we finally obtain the energy balance of the steady-state column in cylindrical coordinates as

$$\sigma E^2 + \frac{1}{r}\frac{d}{dr}(r\kappa\frac{dT}{dr}) - 4\pi\epsilon_N = 0 \tag{7}$$

Eq. (7) is known as the Elenbaas-Heller equation. Its boundary conditions are $dT/dr = 0$ at r=0, and $T = T_w$ at the tube radius r=R. The walls' temperature is taken as 300 K in this whole study. The electric control parameter here is the electric field rather than the current for the sake of simplicity, derived using

$$I = 2\pi E \int_0^R \sigma(T) r dr \tag{8}$$

Any electric circuit model is needed since the arc impedance is assumed to be small compared to the combined impedance of the rest of the circuit. Then, the Elenbaas-Heller equation together with Eq. (8) permits calculations of the electric characteristic $E(I)$ of the plasma column.
In addition to the net emission coefficient ϵ_N and as shown in Eq. (7), this solution requires knowing the following material functions: electrical conductivity $\sigma(T)$ and thermal conductivity $\kappa(T)$, plotted in figures 1a and 1b. The plasma characterization will consist firstly in determining

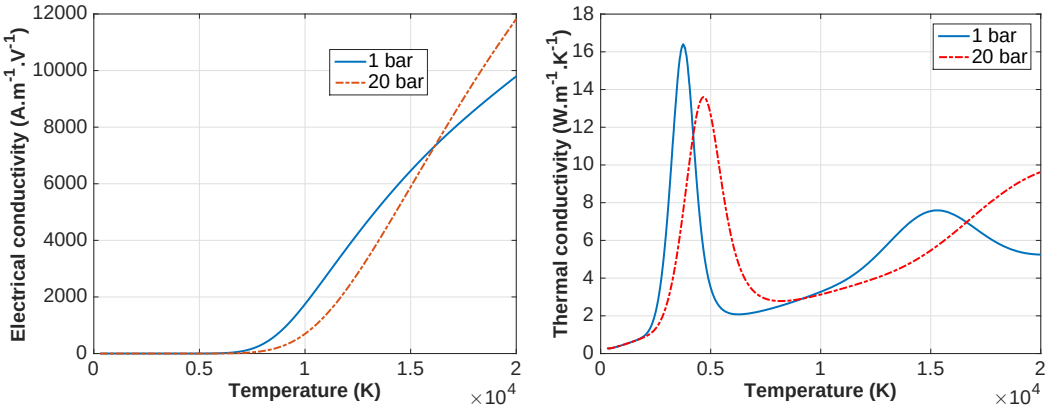

(a) (b)

Figure 1: Electrical and thermal conductivities of hydrogen

these functions from the chemical composition: a calculation code TT Winner [16] based on the Gibbs free energy minimization is used with the temperature ranging from 300 K to 20 000 K and for 1 and 20 bar pressure. As a second step, the transport properties are computed from the composition of the plasma with the Chapman-Enskog approach [17] which is based on the solution of the integro-differential equation of Boltzmann. Corrections to ideal gas law are also considered: a second order Viriel correction which uses Hirschfelder's formulation [18] and a Debye correction to take into account appearing Coulomb interactions that cause a lowering of pressure [18, 19].
The numerical solutions of Eq. 7 were obtained using an ordinary differential solver in the software MATLAB [20]. Once the dependencies of net emission coefficient, thermal and electrical conductivities on temperature are set up, the algorithm gives the temperature profile and the resulting current for a given value of electric field and a guessed axial temperature T_0. The solution at the tube walls is compared to the specified boundary temperature. If not equal, T_0 is modified and so on, until convergence is achieved.

3.3 Net emission coefficient

In many plasma studies, radiation is neglected or estimated with empirical formulas [10]. However, at high current and/or pressure, it becomes the main heat transfer mechanism [16]. For more accurate results, we consider the following Radiative Transfer Equation (RTE)

$$\vec{n} \cdot \nabla I_\nu = k'_\nu (B_\nu - I_\nu) \tag{9}$$

This manuscript was accepted by J. Appl. Phys. Click here to see the version of record.

where

$$k'_\nu = k_\nu\left[1-\exp(-\frac{h\nu}{kT})\right] \quad (10)$$

$$B_\nu = \frac{2h\nu^3}{c^2}\left[\exp(\frac{h\nu}{kT})-1\right]^{-1} \quad (11)$$

$$J_\nu = \frac{1}{4\pi}\int_{4\pi} I_\nu(\vec{r},\vec{n})d\Omega \quad (12)$$

k'_ν is the absorption coefficient corrected by the induced emission and correlated with the local emission coefficient by the Kirchhoff law; B_ν the Planck function; J_ν the average radiation intensity; I_ν the radiation intensity in the $\vec{r}$ direction, through a surface unit of normal direction $\vec{n}$.

As a simplification, the method of the net emission coefficient (NEC) developed by Lowke [15] is used

$$4\pi\epsilon_N = \nabla\cdot\vec{q}_{rad} \quad (13)$$

$$\vec{q}_{rad} = \int_0^\infty\int_{4\pi} I_\nu(\vec{r},\vec{n})\vec{n}d\Omega d\nu \quad (14)$$

$\vec{q}_{rad}$ being the radiative flux density.

Lowke and Liebermann [21] solved the RTE for two geometries and showed that one can replace, as a first approximation and with 90% accuracy, the radiation calculated at the axis of an isothermal cylinder by the emission at the center of an isothermal and homogeneous sphere of radius R_p. This leads to

$$\epsilon_N = \int_0^\infty k'_\nu B_\nu \exp(-k'_\nu R_p)d\nu \quad (15)$$

The derivation of the net emission coefficient ϵ_N requires to first compute the spectrum of the absorption coefficient k'_ν. This is achieved thanks to the recent work of T. Billoux [8]. It yields to a huge database with a temperature range from 300 to 30.000 K and wavelengths from 0.209 μm to infrared, as shown in figures 2 and 3 (database provided by the LAPLACE laboratory). The radiation from background continuum, either molecular (H_2) or atomic (H, H^- and H^+), from molecular diatomic bands, and from 74 lines spectrum for hydrogen is considered. This huge investigation allows having a more precise calculation of the radiative contribution.

The net emission coefficient method gives a very good estimation of the radiation losses from the hot zones [22]. Self-absorption should be taken into account through the parameter R_p appearing in Eq. (15). ϵ_N corresponds then to the difference between the local emitted radiation and that emitted somewhere else and absorbed locally. Hence, it decreases when the plasma thickness increases as shown in figure 4. However, the authors are aware of certain inherent limitations of NEC approach: the divergence of radiative flux is always positive whereas the radiation will be absorbed by the cold gas surrounding the arc whenever the arc radiation is principally in the far ultraviolet region of the spectrum. At this region, the value of net emission coefficient will be negative [23].

In addition, the determination of the plasma thickness R_p is not straightforward and appears to be a limit when treating the absorption spectrum with either a geometrical simplification through the net emission coefficient or with a spectral simplification like the Planck band-averaged method [24].

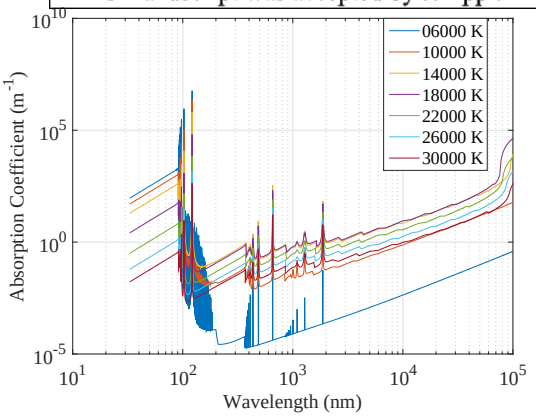

Figure 2: Absorption coefficient of hydrogen plasma at 1 bar

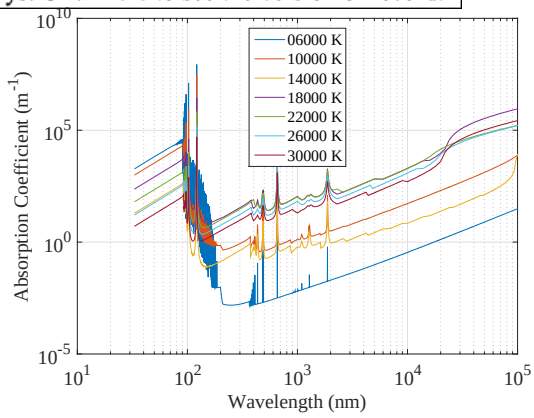

Figure 3: Absorption coefficient of hydrogen plasma at 20 bar

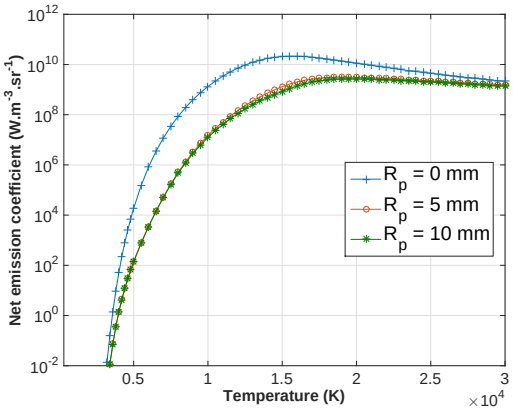

Figure 4: NEC of hydrogen plasma at 1 bar and for different plasma thicknesses

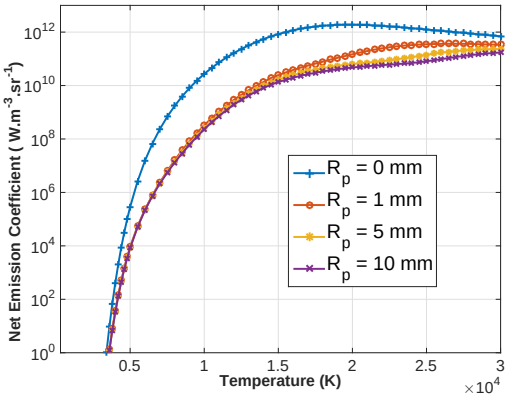

Figure 5: NEC of hydrogen plasma at 20 bar and for different plasma thicknesses

For the cylindrical arc of radius r_0 and temperature T_{arc}, Nordborg et al. [24] achieved satisfactory results compared to experiments by integrating the net emission over the volume of the arc

$$\frac{2}{r_0^2}\int_0^{r_0} r dr \nabla \cdot \vec{q}_{rad} = \frac{2\pi B_\nu}{r_0} S_{exact}(k'_\nu r_0) \tag{16}$$

where $2\pi B_\nu / r_0$ is the black body net emission, S_{exact} is the dimensionless form factor. The computation of the latter is somewhat complicated, even for the cylindrical arc, but a reasonably good approximation is found in Eq. 17

$$S_{exact} \approx 1 - \exp(-2x) \tag{17}$$

which is exactly valid for small and large $x = k'_\nu r$ (with the arc behaving as a black body when the absorption is strong, $S_{exact} \to 1$) and interpolates nicely for intermediate values.

Hence, R_p which helps better handling peaks in the absorption spectrum, can be fairly approximated with $2r_0$ in this study, provided that the arc radius r_0 can be obtained for a specified

pressure, current and the tube geometry. Besides experiments, this can be done in an original way presented in the next lines.

3.4 Semi-analytic solution

In this section, we rewrite the Elenbaas-Heller equation Eq. (7) in order to find an analytic solution and determine the arc radius (and consequently the plasma thickness $R_p = 2r_0$) for a better computation of the radiative term in cylindrical arcs. Analytic analysis of this equation have been given in some papers: Maecker [25] for the constricted type arc where radiation was neglected; Shaw [26] for the same case but using the regular perturbation theory up to the second order whereas Kuiken [7] worked on a radiating wall-stabilized high-pressure gas discharge arc with an asymptotic treatment to yield an explicit expression linking the arc current to the maximum arc temperature. Unlike the previously cited authors, we do not consider the electrical conductivity as a temperature rule based on the Saha equation (with the accounting of its nonlinear characteristics by Arrhenius-type function), neither the thermal conductivity in a power form of temperature.
The use of heat flux potential has greatly simplified analytic investigations on arc problems [26,27] .

$$S(T) = \int_{T_{ref}}^{T} \kappa(\alpha) d\alpha \tag{18}$$

All other thermodynamic, radiative and transport properties should be expressed in terms of S. For the electric conductivity σ , Schmidt [28] suggested to take it zero until a cut-off value S_1 before it rises linearly with a best-fit slope to the highest value which occurs in the arc column.

$$\begin{aligned} \sigma &= 0 \quad if \quad S \leq S_1 \\ \sigma &= B(S - S_1) \quad else \end{aligned} \tag{19}$$

This is in satisfactory agreement with figure 6 and with the physics of the cooled arc. Indeed, a piece-wise function for the conductivity refers naturally to an arc with a conductive zone close to the axis (on an arc radius r_0) and a non-conductive outer region where Joule heating can be fairly neglected.

The energy equation is written as

$$\begin{aligned} E^2 B(S - S_1) + \frac{1}{r}\frac{\partial}{\partial r}\left(r\frac{\partial S}{\partial r}\right) - 4\pi\epsilon_N(S) &= 0 \quad for \quad 0 \leq r \leq r_0 \\ \frac{1}{r}\frac{\partial}{\partial r}\left(r\frac{\partial S}{\partial r}\right) - 4\pi\epsilon_N(S) &= 0 \quad for \quad r_0 \leq r \leq R \end{aligned} \tag{20}$$

with the following auxiliary conditions

$$S(r_0^+) = S(r_0^-) = S_1, \quad S(R) = S_2, \quad S_r(r_0^+) = S_r(r_0^-) \quad and \quad S_r(0) = 0 \tag{21}$$

where the superscripts - and + refer respectively to the solutions in the conductive and non-conductive regions.
We fix the free boundary at the two regions by defining

$$\begin{aligned} x &= r/r_0 \quad for \quad 0 \leq r \leq r_0 \\ y &= (R - r)/(R - R_0) \quad for \quad r_0 \leq r \leq R \end{aligned} \tag{22}$$

And we make the dependent variables dimensionless through

$$\begin{aligned} U &= (S - S_1)/(S_1 - S_2) \quad for \quad 0 \leq r \leq r_0 \\ V &= (S_1 - S)/(S_1 - S_2) \quad for \quad r_0 \leq r \leq R \end{aligned} \tag{23}$$

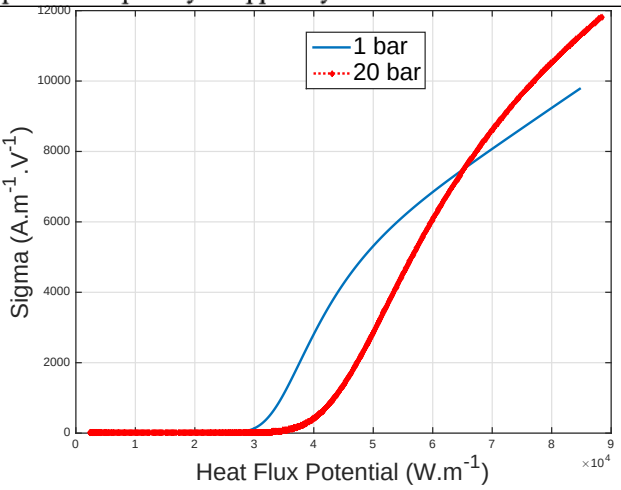

Figure 6: Electric conductivity with heat flux potential of hydrogen

One can introduce finally the dimensionless factors of the arc radius, the electric field strength, the current and the net emission coefficient respectively

$$\rho = r_0/R, \quad E^* = B^{1/2}RE, \quad I^* = I/(S_1 - S_2)RB^{1/2} \quad and \quad \epsilon_N^* = 4\pi R^2 \epsilon_N/(S_1 - S_2) \tag{24}$$

After some mathematical transformations, the previously described dimensional boundary value problem becomes

$$\begin{aligned} \rho^2 E^{*2} U + \frac{1}{x}\frac{\partial}{\partial x}\left(r\frac{\partial U}{\partial r}\right) - \rho^2 \epsilon_N^*(U) &= 0 \quad for \quad 0 \le x \le 1 \\ \frac{d^2V}{dy^2} - \frac{1}{\left[(1-\rho)^{-1} - y\right]}\frac{dV}{dy} - (1-\rho^2)\epsilon_N^*(U) &= 0 \quad for \quad 0 \le y \le 1 \end{aligned} \tag{25}$$

with the following boundary conditions

$$U(1) = 0, \quad U_x(0) = 0, \quad V(1) = V(0) = 0, \quad U_x(1) = \frac{\rho}{1-\rho} V_y(1) \tag{26}$$

while Ohm's law reduces to

$$I^* = 2\pi\rho^2 E^* \int_0^1 xU(x)dx \tag{27}$$

3.4.1 Radiation negligible

When radiation is negligible (small current and low pressure cases for instance), an analytic solution is easily achievable. The dimensionless form of the energy equation in the inner region results in a Bessel equation of the type

$$\frac{d^2U}{dx^2} + \frac{1}{x}\frac{dU}{dx} + \left(\rho E^*\right)^2 U = 0 \tag{28}$$

and which solution is in the form

$$U(x) = aJ_0(\rho E^* x) + bY_0(\rho E^* x) \tag{29}$$

where J_0 and Y_0 are respectively the first Bessel functions of first and second kinds. With the boundary conditions, the inner solution is

$$U(x) = U_m J_0(\rho E^* x) \tag{30}$$

with

$$\beta = \rho E^* \tag{31}$$

the first zero of the Bessel function J_0 .
The solution at the outer region is straightforward

$$V(y) = U_m \beta J_1(\beta) \log\left[\frac{1-(1-\rho)y}{\rho}\right] \tag{32}$$

Using the boundary condition at the edge of the conducting zone and Ohm's law, we have the following expressions to close the problem

$$U_m = \frac{1}{\beta J_1(\beta)\log(1/\rho)} \tag{33}$$

$$I^* = \frac{2\pi}{\beta}\frac{\rho}{\log(1/\rho)} \tag{34}$$

3.4.2 Radiation not negligible

The difficult task for the radiative case is the modeling of the net emission coefficient as a function of the heat flux potential. Such achievement represents one originality of this present work. Figure 7 suggests a linear piece-wise function as for the electric conductivity. Radiation can be taken zero in the non-conductive region that corresponds to low temperature and linearly dependent of the heat flux potential in the inner region.

Hence we rewrite the net emission coefficient in the form

$$\epsilon_N^* = {E_+^*}^2 U \tag{35}$$

where the subscript+ refer to an additional contribution of radiation the electric field. Solutions are still given by Eq. (30) and Eq. (32) but with new formulas for E^*, U_m and I^*

$$E^* = \frac{\beta}{\rho}\sqrt{1+\left(\frac{\rho E_+^*}{\beta}\right)^2} \tag{36}$$

$$U_m = \frac{1}{\beta J_1(\beta)\log(1/\rho)} \tag{37}$$

$$I^* = \frac{2\pi}{\beta}\frac{\rho}{\log(1/\rho)}\sqrt{1+\left(\frac{\rho E_+^*}{\beta}\right)^2} \tag{38}$$

In addition to this general expressions, we derive from Eq. (38) the arc radius r_0 for a given pressure, current and geometry. Actually, the slope of the dimensionless net emission coefficient E_+^* is a function of

$$R_p \approx 2r_0 \tag{39}$$

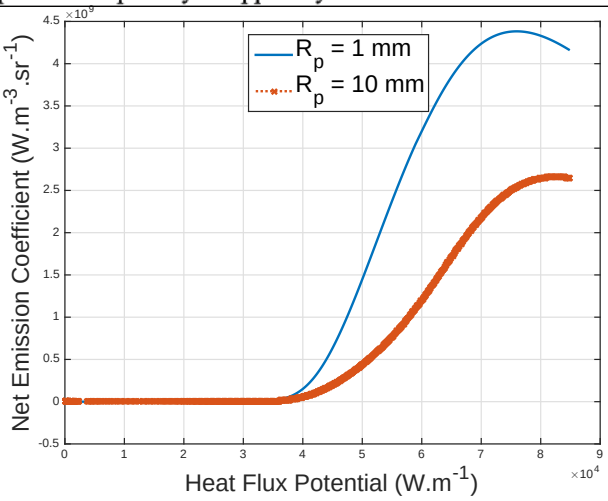

Figure 7: Net emission coefficient with heat flux potential of hydrogen at 1 bar

Figure 8 shows that, for a current of 200 A, the arc diameter is nearly 6 mm at 1 bar whereas at 20 bar, more constriction is observed with a 3 mm arc diameter. This is a well-known effect of pressure in an arc and is in agreement with one can expect intuitively. It is also validated by experimental works on hydrogen Huels-type arc heater done by Painter et al. [29] and which give an arc radius of the order of millimeter for 20 atm operating pressure. The difference may be explained by the fact that convection, which constricts the arc, is not considered in our study whereas the arc was blown in the experimental case.

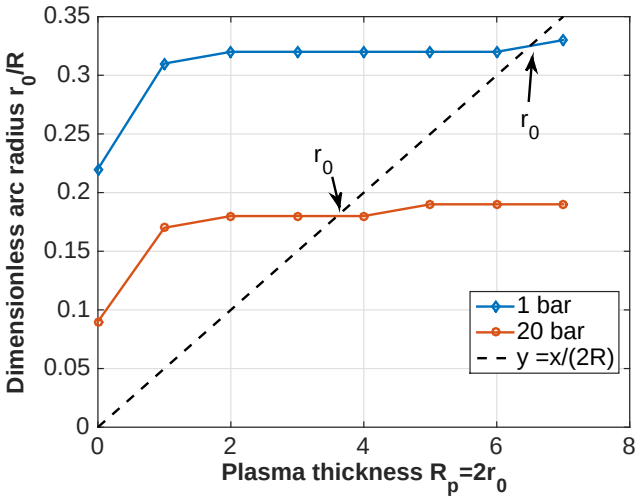

Figure 8: Determination of the arc radius r_0 indicated by the arrows, at 1 and 20 bar for I=200 A and R=10 mm tube radius

4. Results

4.1 Temperature profiles

With a homemade MATLAB code, we derive, from the Elenbaas-Heller equation, the temperature profile for a given electric field and pressure. The difficult part of the calculation was to enforce the boundary condition at the wall as the latter is in fact a strong function of the core temperature. Once a self-consistent solution was reached, we can generate a family of temperature profiles presented in figure 9.

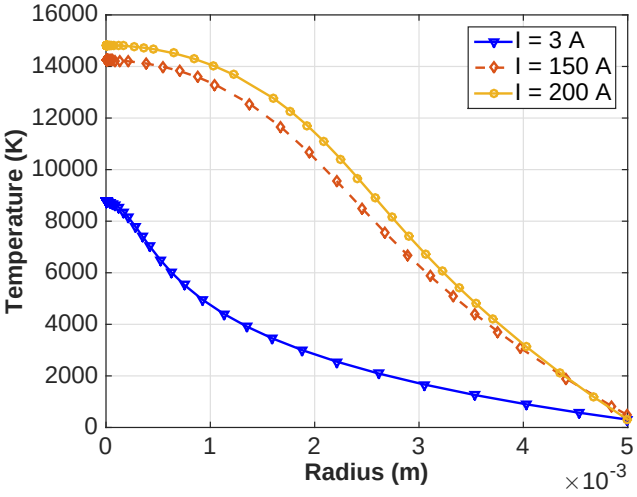

Figure 9: Radial distribution of temperature of a wall stabilized arc column of 5 mm tube radius at 1 bar and considering R_p=4 mm

It can be seen a surge in the core temperature when current increases up to 200 A. Moreover, at high current and temperature, the distribution becomes much squarer, going from a core profile with high gradient to a coreless form. This change can be interpreted going back to the Elenbaas-Heller equation, with a changing mechanism of heat loss.
The primary information on the radial distribution of temperature follows from the differential equation of energy at the axis:

$$-2\kappa \frac{d^2T}{dr^2}|_{r=0} = \sigma_0 E^2 - S_{rad_0} \tag{40}$$

where $\sigma_0 = \sigma(T_0)$, $S_{rad_0} = \nabla \cdot \vec{q}_{rad}(T_0)$, $T_0 = T(r = 0)$.
Eq. (40) shows that the sign of $\sigma_0 E^2 - S_{rad_0}$ determines the one of the second derivative of the temperature, hence the sign of the curvature of the profile in the immediate vicinity of the arc axis. The assumption of the maximum temperature at the axis of the arc indicates that the strength of the electrical field should satisfy the following condition

$$E^2 > S_{rad_0}/\sigma_0 \tag{41}$$

The profile $T(r)$ strongly depends on the nature of variation of the complex S_{rad_0}/σ_0 with temperature [15]. At low temperature, it is low due to small radiation losses and the temperature

profile must have a large enough gradient to drive the conductive losses. The arc consists then of a narrow central core with a sharp decrease of temperature, i.e. the constricted type arc. At high temperatures, S_{rad_0}/σ_0 is great and sufficient heat can be radiated without a large temperature gradient. Thus, as the core temperature increases, the profile becomes flatter in the center and squarer in shape.

It is also useful to note that, at current of hundreds amperes, a little change of the core temperature can lead to a swing with a temperature increasing radially (that is a heat input is required from the outside). This is probably due to the strong temperature dependence of the radiative losses, especially at 20 bar where the condition stated by Eq. (41) implies to consider absolutely auto-absorption (R_p different of zero) to avoid this swing and have a physical solution.

4.2 Current-voltage characteristic

From the derived temperature profile, the computation of the current with Eq. (8) is a straightforward integration.

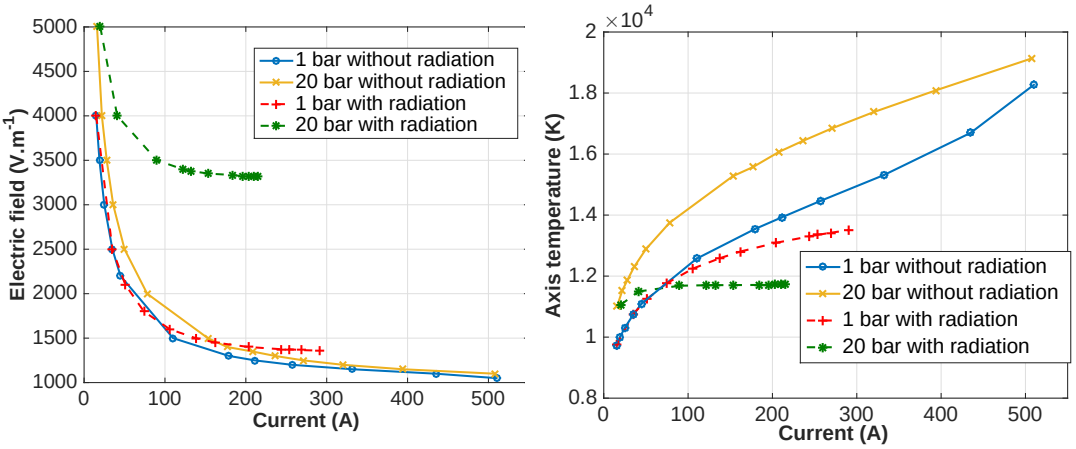

(a) Electric characteristic

(b) Temperature at the axis

Figure 10: Current-voltage characteristic and axis temperature of a wall stabilized arc column of 10 mm radius: $R_p = 6$ mm at 1 bar and 4 mm at 20 bar when radiation is considered

It comes out from figure 10.a that the electric field is decreasing with current. The hyperbolic form of the plots suggests that the power per unit length EI is almost constant in the current range considered here. At 1 bar pressure, radiation can be negligible until a current of the order of one hundred amperes whereas at 20 bar, it becomes preponderant even at very low current. We observe also from figure 7.b that the temperature of the arc decreases with radiation, especially at 20 bar.

These remarks on the pressure were regardless the confinement. In fact, reducing it was only responsible of a decrease in the electric field at a given current. This is due to the conjunction of a cooling of the arc and a modification in the temperature profile, from a constricted type arc to an arc flatter at the center (see figures 11 and 12).

For the hydrogen arc plasma at 20 bar and nearly 220 A current, we obtained a maximum temperature of 11250 K and an electric field E= 3300 $V.m^{-1}$ with $\approx$ 3.5 mm arc diameter. This is a satisfactory agreement with the work of Painter [29] except for the electric field (see Table 1). The discrepancies are due to the fact that convection losses are not considered in this present

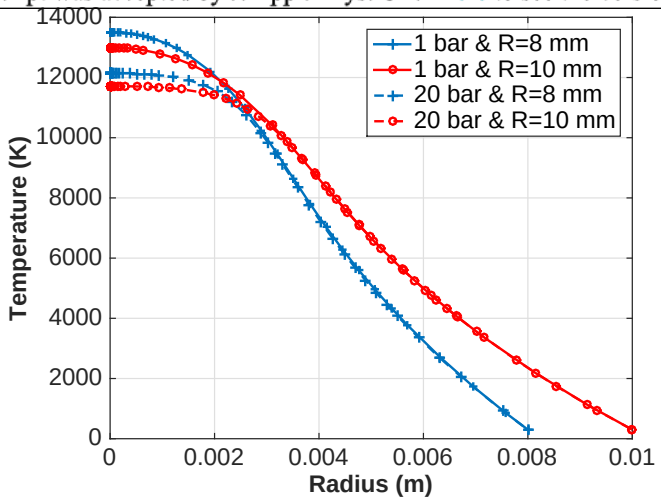

Figure 11: Radial distribution of temperature of a wall stabilized arc column for different radii, I=195A and at 1 bar and 20 bar

I (A)	240	320	400
Arc temperature (K)	11475	11562	11662
Arc diameter (mm)	4.2	4.8	5.2
Electric field ($V.m^{-1}$)	8300	8140	7951

Table 1: Performances for a 20 bar hydrogen plasma arc with a 0.375 inch ($\approx$ 9.5 mm) constrictor [29]

paper as they would have increase consequently the electric field.
On the pressure effect, it comes from figures 10.a, 12 that changing operational conditions from 1 to 20 bar leads to an electric field multiplied by a factor between 2 and 3 (the upper limit was obtained for the smallest value of tube radius 5 mm) for a current of 200 A (here we speak strictly of pressure dependence; as already stated, the gas flow rate obviously has its own dependency, that is out of the scope of this paper). This is the order of magnitude found with empirical laws given in the literature regarding the effect of pressure on hydrogen blown arcs [4,9] respectively:

$$E \propto P^{0.4} \tag{42}$$

$$E = Alog(P) + B \tag{43}$$

and for which the multiplying factor is around 3.

4.3 Semi-analytic solutions

While numerical solutions are widely used nowadays thanks to huge computational resources, they generally have some parameters that can be set up thanks to analytic solutions. As aforementioned, the plasma thickness R_p appearing in the net emission coefficients calculation is one these parameters and the semi-analytic solutions developed in section 3.4 for cylindrical arcs enable to fix it more precisely.
Figure 13.a shows that the analytic results for the electric characteristic compare relatively well with the numerical solutions. There is less than 5% difference in the axis temperature of the two

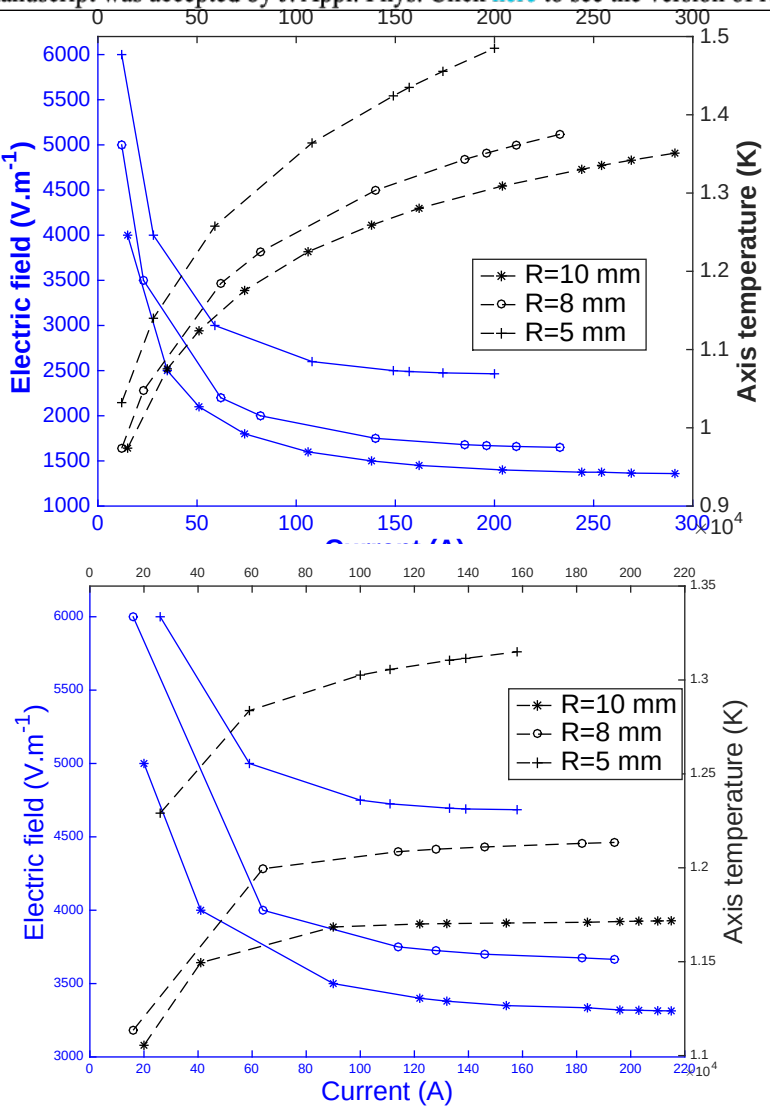

Figure 12: Electric characteristic and temperature at the axis vs current for a wall stabilized arc column: 1 bar (top) and 20 bar (bottom)

solutions.

In fact, the voltage of a wall-stabilized cylindrical arc is mainly dependent on the near axis phenomena as shown in figure 13.b. The arc radius model (as specified in section 3.4 through a conductive and a non-conductive zones) is sufficient to capture such phenomenon, with a good estimation of the temperature distribution in the inner region despite discrepancies in the outer zone.

Regarding the prediction of pressure effect on power per unit length, we obtain from Eq. 31, 34,

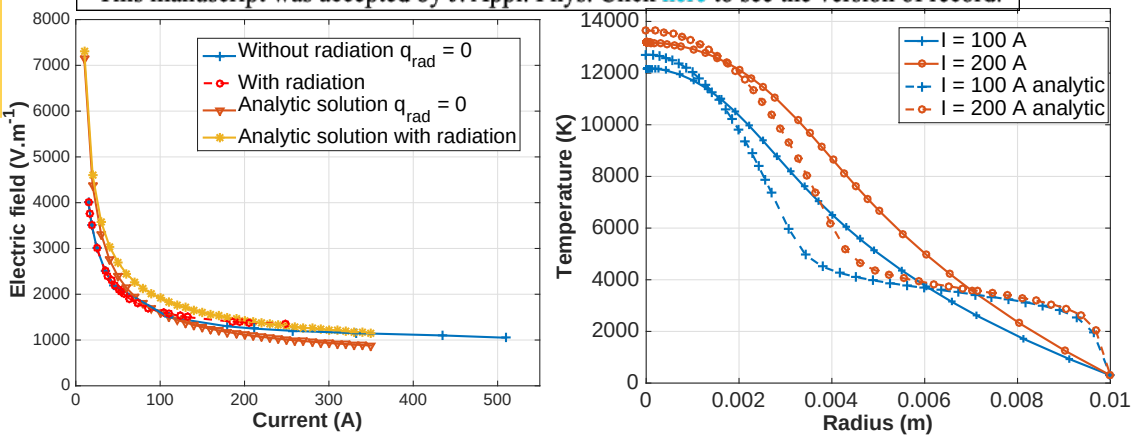

(a) Electric characteristic

(b) Temperature profile

Figure 13: Electric characteristic and temperature profile of a wall stabilized arc column of 10 mm radius at 1 bar and $R_p = 6$ mm

36 and 38 and after going back to dimensional values

$$\frac{(EI)_{20bar}}{(EI)_{1bar}} = \frac{\log(1/\rho_1)}{\log(1/\rho_{20})}\left[1+\left(\frac{\rho_{20}(E_+^*)_{20}}{\beta}\right)^2\right]\left[1+\left(\frac{\rho_1(E_+^*)_1}{\beta}\right)^2\right]^{-1}\frac{(S_1-S_2)_{20}}{(S_1-S_2)_1} \qquad (44)$$

with the notations given in section 3.4. With the values specified in Table 2, we evaluate the ratio

	S_1	S_2	ρ	β	E_+^*
1 bar	$3.06e4$	0	0.32	2.4048	7-8
20 bar	$4.12e4$	0	0.18	2.4048	34-37

Table 2: Values for analytic solutions of the hydrogen arc at 200 A in 10 mm cylindrical tube

of power per unit length when the pressure raises from 1 to 20 bar (Eq. 44): it ranges between 3.12 to 4.13, which is in satisfactory agreement with the results and the conclusions in section 4.2.

The effect of confinement was also predictable analytically, with the change in the profile of temperature from a constricted type arc to a flatter-at-the-center arc when radius R is increased (figure 14). This confinement reaches a limit from which the arc radius does not vary much despite an increased tube radius: twice less confinement (with R from 15 to 30 mm) results in less than 7% change in arc maximum temperature. Then one can consider the arc to burn freely for R bigger than 15 mm (tube walls have no more substantial effect). This value is in agreement with the results of experimental investigations on hydrogen plasma [9].

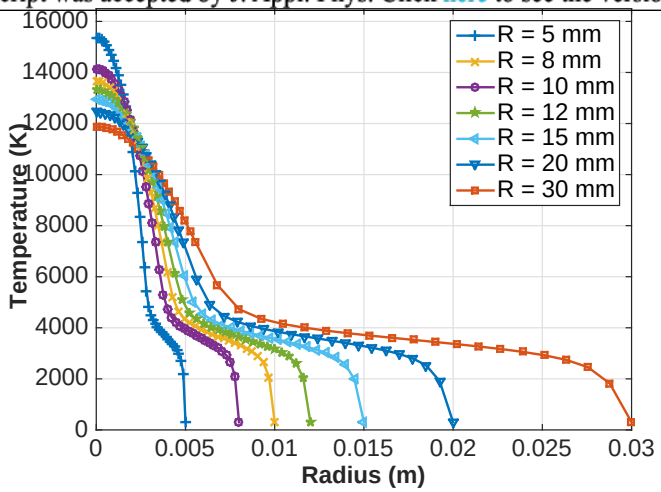

Figure 14: Confinement effect on analytic temperature profiles of a wall stabilized arc column at 1 bar and I = 200 A

Concluding remarks

The arc column model developed in this paper gives numerical and analytic results that are in satisfactory agreement with previous works on hydrogen current-voltage characteristic [4, 9]. It confirms a multiplying factor of around 3 when pressure is raised from 1 to 20 bar and for a current of around 200 A and corroborates the fact that, in high temperature plasma due to current and/or pressure increase, the radiation induces an important energy loss that must be taken into account in any model. It is thus crucial to have a proper treatment of the radiative heat transfer in any high pressure/current simulations.

For the net emission coefficient's method used to include radiation, the plasma thickness is a parameter that one cannot always specify exactly and which affects the results. The analytic solving of our cylindrical arc allows us to determine it more precisely. The modeling of electric conductivity and net emission coefficients by piece-wise linear functions of the heat flux potential is one originality of this research.

However, the method of net emission coefficient reaches its limit when the arc is less and less confined. Then, absorption at the edge has to be considered, through an exact 1D resolution of the radiative transfer equation for instance. Work is in progress toward the integration of this phenomenon and comparisons with results presented herein would be of great interest in a next paper.

Finally, as with any physical modeling process, trade-offs must be made between solving simpler models that include the principal physical processes (and hence more cost-effective) and solving more detailed models which may include parameters only vaguely known. Thus simpler approaches, particularly when correlated with validated data, can often be adequate for engineering estimation purposes. Even if a plasma arc is in reality blown and not confined and undergoes convective losses, this work based on a channel arc model and semi-analytic models can bring very fruitful information for the scientific community at a lesser cost, particularly regarding basic process design: it gives the appropriate tendencies for the electric characteristic, which is crucial in the specification of a plasma reactor power supply.

Bibliography

[1] L. Fulcheri, N. Probst, G. Flamant, F. Fabry, E. Grivei, and X. Bourrat. Plasma processing: a step towards the production of new grades of carbon black. *Carbon*, 40(2):169–176, 2002.

[2] F. Fabry, G. Flamant, and L. Fulcheri. Carbon black processing by thermal plasma. analysis of the particle formation mechanism. *Chemical Engineering Science*, 56(6):2123–2132, 2001.

[3] C. Rehmet. *Étude théorique et expérimentale d'une torche plasma triphasée à arcs libres associée à un procédé de gazéification de matière organique*. Thesis, 2013. Thèse de doctorat Energétique et Procédés Paris, ENMP 2013 2013ENMP0041.

[4] R. Philips et al. Three-phase ac arc heater. Technical report, ARL 64-29, Aerospace Reasearch Laboratories, US Air Force, 1964.

[5] G. Saevarsdottir, H. L. Larsen, and J. A. Bakken. Modelling of industrial ac-arcs. *High Temperature Material Processes*, 3(1):1–15, 1999.

[6] H. A. Stine and V. R. Watson. The theoritical enthalpy distribution of air in steady flow along the axis of a direct current. Technical report, NASA Technical Note D-1331, 1962.

[7] H. K. Kuiken. An asymptotic treatment of the elenbaas-heller equation for a radiating wall-stabilized high-pressure gas-discharge arc. *Journal of Applied Physics*, 70(10):5282–5291, 1991.

[8] T. Billoux, Y. Cressault, and A. Gleizes. Net emission coefficient for co–h2 thermal plasmas with the consideration of molecular systems. *Journal of Quantitative Spectroscopy and Radiative Transfer*, 166:42–54, November 2015.

[9] M. F. Zhukov. *Thermal plasma torches*. CISP, 1975.

[10] V. L. Granovsky. *Electric current in gas*. Nauka, 1971.

[11] V. Nemchinsky. Modeling arc in transverse magnetic field by using minimum principle. *IEEE Transactions On Plamsa Science*, 44(11), 2016.

[12] M. S. Benilov and G. V. Naidis. What is the mathematical meaning of steenbeck's principle of minimum power in gas discharge physics? *Journal of Physics D-Applied Physics*, 43(17), 2010.

[13] W. Elenbaas. *The High Pressure Mercury Vapour Discharge*. North-Holland, 1951.

[14] H. Maecker. Plasmastromungen in lichtbogen infolge eigenmagnetischer kompression. *Zeitschrift Fur Physik*, 141(1-2):198–216, 1955.

[15] J. J. Lowke. Characteristics of radiation-dominated electric arcs. *Journal of Applied Physics*, 41(6):2588–2599, 1970.

[16] B. Pateyron. *Contribution à la réalisation et à la modélisation de réacteurs plasmas soufflés ou transférés appliqués à la métallurgie extractive et à la production de poudres ultrafines métalliques ou céramiques*. Thesis, Université de Limoges, 1987.

[17] S. Chapman and T. G. Cowling. *The mathematical theory of non uniform gases*. New-York: Cambridge university press, 1952.

[18] O. Hirschfelder, F. Curtis Charles, and R. Bird. *Molecular theory of gases and liquids*. John Wiley and sons, 1964.

[19] H. R. Griem. *Plasma spectroscopy*. McGraw Hill, 1964.

[20] MATLAB. *version 7.10.0 (R2010a)*. The MathWorks Inc., Natick, Massachusetts, 2010.

[21] R. W. Lieberman and J. J. Lowke. *J. Quant. Spectrosc. Radiat. Transfer*, 9:207, 1969.

[22] Y. Cresault and A. Gleizes. Thermal plasma properties for ar-al, ar-fe and ar-cu mixtures used in welding plasmas processes: I. net emission coefficients at atmospheric pressure. *Journal of Physics D-Applied Physics*, 2013.

[23] P. Kovitya and J. J. Lowke. 2-dimensional analysis of free burning arcs in argon. *Journal of Physics D-Applied Physics*, 18(1):53–70, 1985.

[24] H. Nordborg and A. A. Iordanidis. Self-consistent radiation based modelling of electric arcs: I. efficient radiation approximations. *Journal of Physics D-Applied Physics*, 41(13):10, 2008.

[25] H. Maecker. *Zeitschrift Fur Physik*, 157(1), 1959.

[26] B. D. Shaw. Regular perturbation solution of the elenbaas-heller equation. *Journal of Applied Physics*, 99(3):6, 2006.

[27] G. Schmidt. Zur therorie der wandstabilisieren bogensaule. *Zit. Naturforschung*, 5a:571, 1950.

[28] G. Schmidt, H. J. Patt, and J. Uhlenbusch. Eigenschaften und parameterabhängigkeit der temperaturverteilung und der characketiristik eines zyylindersymmetrischen stickstoffbogens. *Zeitschrift für Physik*, 173:552–567, 1963.

[29] J. H. Painter. Performance characteristics of a huels-type arc heater operating on hydrogen, helium or air. Technical report, McDonnell Douglas Research laboratories AD, March 1976.